Astron. Astrophys. 360, 647–655 (2000)

ASTRONOMY AND ASTROPHYSICS

WN stars in the LMC: Parameters and atmospheric abundances

W.-R. Hamann and L. Koesterke

Lehrstuhl Astrophysik, Universität Potsdam, Am Neuen Palais 10, 14469 Potsdam, Germany (wrh@astro.physik.uni-potsdam.de)

Received 17 April 2000 / Accepted 7 June 2000

Abstract. The spectra of 18 WN stars in the Large Magellanic Cloud (LMC) are quantitatively analyzed by means of "standard" Wolf-Rayet model atmospheres, using the helium and nitrogen lines as well as the spectral energy distribution. The hydrogen abundance is also determined. Carbon is included for a subset of 4 stars. The studied sample covers all spectral subtypes (WN2... WN9) and also includes one WN/WC transition object.

The luminosities of the program stars span a wide range ($\log L/L_\odot$ = 5.0... 6.5). Due to the given LMC membership, these results are free from uncertainties inferred from the distance. 50% of the studied stars (both, late and early WN subtypes) have rather low luminosity ($\log L/L_\odot \leq 5.5$). This puts tough constraints on their evolutionary formation. If coming from single stars, it provides evidence for strong internal mixing processes.

The empirical mass-loss rates are scaled down by a factor of about two due to the impact of clumping, compared to previous studies adopting homogeneous winds. There is no obvious strong correlation between the mass-loss rates and other parameters like luminosity, temperature and composition.

The stellar parameters for the present LMC sample are not systematically different from those of the Galactic WN stars studied previously with the same techniques, in contrast to the expected metallicity effects.

Key words: stars: atmospheres – stars: fundamental parameters – stars: Wolf-Rayet – galaxies: individual: LMC

1. Introduction

The Wolf-Rayet (WR) stars play a key role for unraveling the evolution of massive stars, as well as for the understanding of the physics in strong stellar winds. The analyses of their spectra provide the main empirical access to these questions.

Most previous work focused on Galactic WR stars. The LMC objects studied in the present paper deserve our interest for two reasons. Firstly, the evolution of massive stars is predicted to differ from our Galaxy, mainly because the lower metallicity in the LMC should lead to smaller radiation-driven mass-loss. Secondly, some of the basic stellar parameters, especially the luminosity, require knowledge of the stellar distance for being determined spectroscopically. LMC members have the great advantage that their distance is a priori known.

WR spectra are characterized by broad emission lines and are formed in rapidly expanding stellar winds under extreme non-LTE conditions. Their analysis requires adequate model atmospheres, which have been developed during the last 15 years with increasing degree of sophistication.

The first generation of WR model atmospheres was restricted to pure helium composition. A grid of corresponding models was established by Schmutz et al. (1989) and applied to the complete Galactic WN sample (Hamann et al. 1993). 19 WN stars in the LMC have been studied in the same way by Koesterke et al. (1991). The hydrogen abundance in the Galactic WN stars was estimated by Hamann et al. (1995). Improved model atmospheres which account for nitrogen have been employed for analyzing the Galactic WN stars, leading to a partial revision of their parameters (Hamann & Koesterke 1998a). The present work now aims at an analysis of a broader LMC WN sample by means of the more advanced (nitrogen) models, including the determination of the hydrogen abundances.

A model atmosphere code similar to ours has been developed independently by Hillier (e.g. 1987a,b) and extensively applied for spectral analyses of individual WR stars in both our Galaxy and the LMC. The results by Crowther et al. (1995a,b) and Crowther & Smith (1997) will be included in our discussion and compared with our analyses for those six stars which are in common with our sample.

The analytical work hitherto concentrates on the WN class, while comprehensive studies of the WC stars are still lacking. The reason is the poor consistency between synthetic and observed WC spectra encountered (e.g. Hamann et al. 1992). The recent line-blanketed model atmospheres now promise a better agreement (Hillier & Miller 1998, Gräfener et al. 2000), hopefully allowing for a systematic study of the WC class in the near future.

In the following section we briefly describe the applied model atmospheres. The studied sample of stars and the observational data are introduced in Sect. 3, while in Sect. 4 we

Send offprint requests to: W.-R. Hamann

explain how our analyses were performed. The results are presented and discussed in the final section (Sect. 5).

2. The models

2.1. Basic assumptions

A "standard" WR atmosphere is assumed to be spherically-symmetric, homogeneous and stationary. The usual β-law with $\beta = 1$ is adopted for the expansion velocity. The "stellar radius" R_*, which is the inner boundary of our model atmosphere, corresponds per definition to a Rosseland optical depth of 20. The "stellar temperature" T_* is defined as the effective temperature referred to that radius R_*.

Any particular WR atmosphere thus is specified by its basic parameters T_*, R_*, $\dot{M}$, v_∞ and chemical composition (given e.g. as mass fractions $X_{\rm He}$, $X_{\rm N}$ etc.).

Schmutz et al. (1989) discovered an approximate degeneracy in this parameter space. They defined a so-called transformed radius $R_{\rm t}$ (see below) and found that models with same $R_{\rm t}$ exhibit almost the same emission line equivalent widths, irrespective of different combinations of $\dot{M}$, R_* and v_∞ (while, of course, T_*, composition etc. are fixed). This (approximate) invariance was validated by various numerical experiments with reasonable accuracy. In a stricter sense, one might compare only models with same terminal velocity v_∞. Then even the line profiles and the total shape of the emergent spectra are invariant for models with same $R_{\rm t}$, except of a scaling of the absolute flux with R_*^2. This property greatly facilitates any spectral analyses.

There are various pieces of evidence that WR winds are actually inhomogeneous. Recent models account for this clumpiness in a first-order approximation (Hillier 1984, Schmutz 1997, Hamann & Koesterke 1998b). The clumps are assumed to fill a volume fraction $f_{\rm V} = D^{-1}$ while the interclump space is void. The parameter D denotes the factor by which the density in these clumps is enhanced over the density of a homogeneous model with same mass-loss rate. This density enhancement D can be incorporated in the scaling invariance of WR atmospheres. Doing so, the definition of the transformed radius reads (Hamann & Koesterke 1998b)

$$R_{\rm t} = R_* \left[\frac{v_\infty}{2500\,{\rm km\,s^{-1}}} \Big/ \frac{\dot{M}\sqrt{D}}{10^{-4}\,M_\odot\,{\rm yr}^{-1}} \right]^{2/3} . \qquad (1)$$

Thus, spectral analyses with 'clumped' models yield smaller mass-loss rates, while other parameters are not affected. In the present study we adopt inhomogeneous winds with $D = 4$ as a typical value for WN stars (Hamann & Koesterke 1998b). Earlier results obtained with homogeneous models can be easily scaled due to this effect.

2.2. The calculations

The radiation transfer is formulated in the comoving-frame of reference (CMF). Doppler broadening by "microturbulence" is generally set to 100 km s^{-1}. The statistical equations balance all relevant radiative and collisional transition rates. We account explicitly for 175 line transitions between 34 non-LTE levels of helium, and 351 lines (90 levels) in the nitrogen model atom (cf. Hamann & Koesterke 1998a). Hydrogen is described by 11 levels with 45 lines if included. For the subset of models with carbon, the latter element is accounted for with 63 levels and 342 lines (cf. Hamann et al. 1992). About 1500 further lines with low f-value are treated in an approximate way, as well as low-temperature dielectronic recombination (N and C) via about 1000 stabilizing transitions from auto-ionizing states. Radiative equilibrium provides a further constraint equation which determines the temperature stratification.

Radiation transfer and rate equations are solved consistently by the method of "iteration with approximate lambda operators". After the non-LTE population numbers have been obtained, the atomic data are further refined by splitting the levels and multiplets in the observed spectral range as far as necessary, and the emergent spectra are calculated in the observer's frame ("formal integral"). Frequency redistribution by electron scattering is taken into account in this step. – More details of our models calculations are given in previous papers (e.g. Hamann et al. 1994).

A recent improvement of WR model atmospheres concerns the (approximate) inclusion of numerous iron lines (Hillier & Miller 1998, Koesterke et al. 2000). The present paper is still based on unblanketed model atmospheres. Our first studies of blanketed models (Hamann et al., in prep.) revealed that the WN results are not severely modified by these effects. However, blanketed models will be important for future investigation of the wind dynamics, because the iron lines accept most of the radiation pressure. Moreover, WC model spectra seem to be more sensitive to iron opacities which influence the atmospheric ionization stratification (Koesterke et al. 2000).

3. Program stars and observational data

The sample of WN stars in the LMC studied in the present paper has been originally selected by Koesterke et al. (1991), who analyzed it by means of pure-helium models. The selection aimed at a coverage of all WN subtypes. The 30 Dor region was excluded from the program, because of the crowding of stars in that field. We preferably selected the brightest one, and one less bright member of each subclass. Thus, our sample is by no means complete or representative in a statistical sense, contrary to our Galactic studies which comprised virtually the whole catalog of known WN stars.

Spectroscopic binaries were excluded from our sample. However, we kept a couple of stars with spectral classification "WN+O" but no convincing evidence that the spectra are really composite: Br 37[1] showed variable radial velocities in spectra taken by A. Moffat (private communication), but the spectrum does not reveal any features which must be attributed to a companion. Br 52 and Br 88 exhibit no radial velocity changes (Moffat, private communication), i.e. there is no evidence for their

[1] Identification of the program stars by their "Br" or "Brey" numbers refers to the catalogue by Breysacher (1981).

Table 1. Parameters of the analyzed WN stars in the LMC

Brey	Spectral subtype†		T_*	R_t	v_∞	X_H	E_{b-v}	M_v	R_*	$\log \dot{M}$	$\log L$	$\frac{\dot{M} v_\infty}{L/c}$	M	Q‡
	Smith 68	SSM 96	[kK]	$[R_\odot]$	[km s^{-1}]	[%]	[mag]	[mag]	$[R_\odot]$	$[M_\odot/\mathrm{yr}]$	$[L_\odot]$		$[M_\odot]$	
(1)	(2)	(3)	(4)	(5)	(6)	(7)	(8)	(9)	(10)	(11)	(12)	(13)	(14)	(15)
1	WN3-s	WN3b	89.1	3.98	1600	0	0.10	-2.9	1.5	-4.8	5.1	9.2	10	2
4	WN2-s	WN2b+OB?	70.8	10.00	1600	0	0.25	-2.7	2.1	-5.2	5.0	4.9	9	4
6	WN2.5-s	WN4b	100.0	2.00	2500	0	0.05	-4.8	2.4	-3.9	5.7	31.6	22	2
12	WN4-s	WN4b	89.1	2.51	1600	0	0.03	-4.1	2.0	-4.3	5.3	15.9	14	1
13	WN8	WN8h	35.5	7.94	900	25	0.06	-6.0	14.1	-4.1	5.4	13.4	16	1
16	WN2.5-s	WN4b+OB?	70.8	10.00	2500	0	0.17	-5.4	7.5	-4.2	6.1	6.3	38	2
24	WN7	WN6h	39.8	15.84	950	40	0.05	-5.4	9.4	-4.8	5.3	4.1	13	1
26	WN7	WN6(h)+abs?	39.8	15.84	1300	30	0.08	-6.1	14.9	-4.3	5.7	6.1	22	3
27	WN3-w	WN3o	79.4	7.94	1400	0	0.12	-4.1	3.5	-4.8	5.7	2.6	20	4
29	WN3/CE-s	WN4b/CE	79.4	6.31	1600	0	0.14	-4.3	4.0	-4.5	5.8	4.5	23	2
37	WN3-w+abs	WN4+OB	79.4	15.84	1600	0	0.12	-4.9	5.9	-4.8	6.1	0.9	38	3
40	WN4-s	WN4b	79.4	6.31	1500	0	0.10	-3.9	3.0	-4.7	5.5	4.6	17	1
47	WN8	WN6h	39.8	15.84	950	40	0.40	-4.8	7.5	-4.9	5.1	4.6	10	2
52	WN4-w+abs	WN4h+abs	70.8	19.95	1500	50	0.10	-4.2	4.7	-5.2	5.7	1.0	22	2
56	WN6-w	WN5o?+OB	44.7	25.12	1600	20	0.27	-5.9	13.3	-4.6	5.8	3.1	25	2
64	WN9	WN9h	31.0	14.12	400	30	0.26	-6.3	19.5	-4.6	5.5	1.6	17	2
85	WN3-4p-s	WN4b	100.0	1.58	2700	0	0.20	-4.3	1.5	-4.0	5.3	66.1	13	2
88	WN4.5-w+abs	WN5+B?	70.8	25.12	2000	30	0.20	-6.3	11.9	-4.6	6.5	0.8	68	3

† Column 2: classification by Conti & Massey (1989) after the scheme of Smith (1968), augmented by us with the indication -s and -w for strong and weak lines, respectively; Column 3: classification by Smith et al. (1996)

‡ Column 15: fit quality, ranging from 1 (very good) over 2 (good), 3 (satisfactory) to 4 (partly discrepant)

binarity. For Br 56 the reason of the 'WN+O" classification in Smith et al. (1996) remains unclear. Br 48 (classification by Smith et al. 1996: WN5o?+B) has a very strange spectrum which does not fit to any of our models; therefore we adopt that this spectrum may be really composite, and exclude this star from our sample, reducing the list of Koesterke et al. (1991) from originally 19 targets to the remaining 18 stars (cf. Table 1).

The optical spectra of our program stars were obtained at the ESO 3.6m telescope with the CASPEC spectrograph in 1989 by U. Wessolowski. It is the same set of data as already employed by Koesterke et al. (1991). The resolution of the echelle spectra (range from 3800 to 7500 Å) of about 1 Å was degraded by subsequent convolution (with a box profile of 3 Å, typically) in order to reduce noise, and the same smoothing was of course applied to the synthetic spectra before the comparison. The spectra were rectified by adjusting low-order polynomials to the continuum from inspection "by eye".

Optical photometric data were taken from Torres-Dodgen & Massey (1988). UV spectra, if available, were retrieved from the IUE data bank taking advantage from the improved NEWSIPS data reduction.

When scaling model fluxes to the photometric observations, we adopt 18.5mag for the distance modulus to the LMC as confirmed from the Cepheid distance scale after HIPPARCOS (Madore & Freedman 1998). The wavelength scale of each observation is corrected for a radial velocity. The average value for the LMC, 250 km s^{-1}, leads to sufficient agreement with the theoretical line positions in all cases, except for Br 52 which requires $v_{\rm rad}$ = 470 km s^{-1} confirming Cowley et al. (1984).

4. The analyses

For each of the program stars, we compare the observation with a couple of calculated spectra by means of plots like the one shown in Fig. 1. The top panel contains calibrated data (IUE spectra and optical photometry). The latter, using the narrow-band system of Smith (1968), are marked by the blocks (the numbers give the magnitudes). The model flux is plotted twice, as pure continuum (dashed) and including the lines (solid). The theoretical fluxes are diluted according the LMC distance modulus and reddened with a suitably adjusted color excess E_{b-v} (cf. Table 1, Column 8). Note that b and v refer to the narrow-band system of Smith (1968) (the equivalent reddening in the Johnson system is E_{B-V} = 1.21 E_{b-v}). We adopt a Galactic foreground reddening with E_{B-V} = 0.03 mag using Seaton's law (Seaton 1979), while the remaining excess is attributed to the LMC reddening law which we adopt from Howarth (1983). The model continuum is finally scaled to the observation by adjusting a suitable logarithmic offset. If not being zero, this empirical parameter *shift* reflects that the stellar radius in the model is not adequate to the radius of the star observed (*shift* = 2 log[$R_*^{\rm star}/R_*^{\rm model}$]). We might then calculate a new model with more adequate parameters (i.e. aiming at *shift* = 0), but as the transformation invariance holds quite accurately this is not always necessary. For convenience we often take advantage of the "transformation law" (Eq. (1)), and translate *shift* into a corresponding corrections of $\dot{M}$ and L (note that *shift* directly gives log $L^{\rm star}$ – log $L^{\rm model}$).

The (reddened and scaled) model continuum is used to rectify automatically the UV parts of the spectra displayed in two

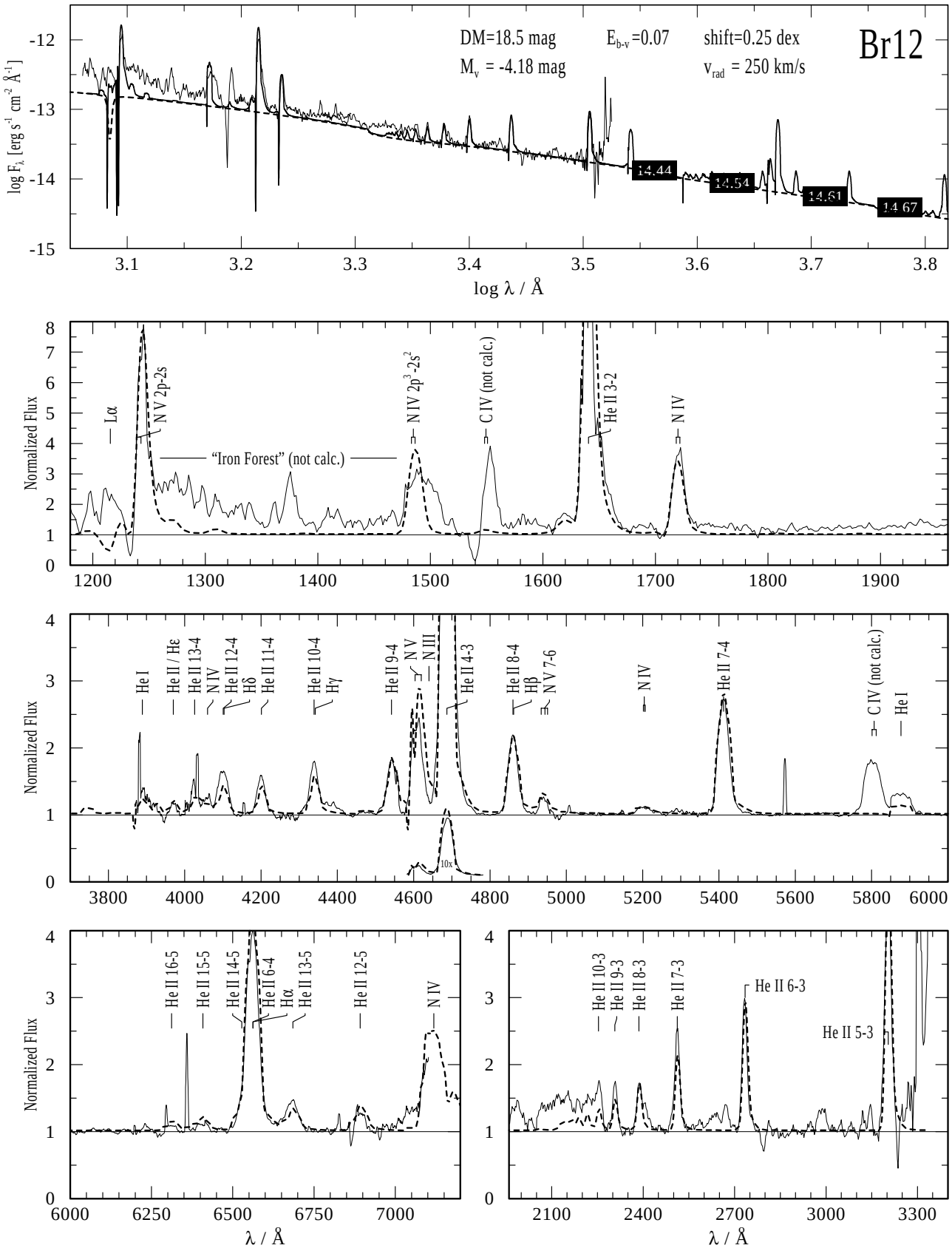

Fig. 1. Spectral fit for Br 12. Thick dashed lines represent calculated spectra, while thin noisy lines are the observation. The uppermost panel shows absolute fluxes in double-logarithmic scale (IUE observation, and photometry). Diagrams of that kind have been applied for the analyses presented in this paper.

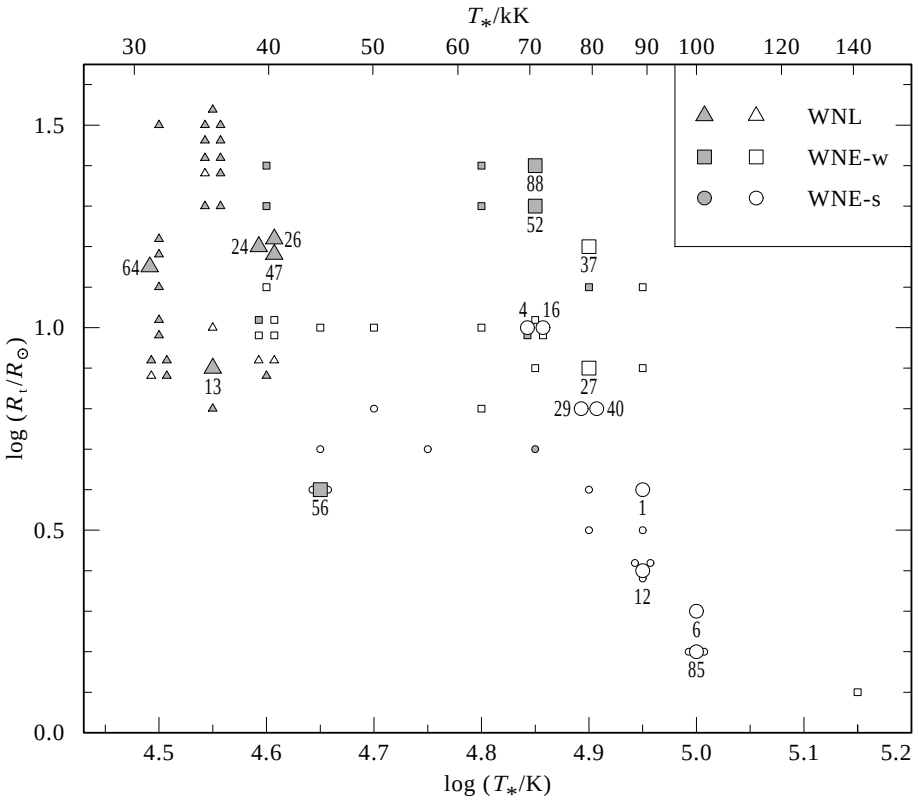

Fig. 2. Positions of the analyzed WN stars in the $\log T_*$-$\log R_t$-plane. The spectroscopic subclasses are distinguished by different symbol shapes (see inset). Filled symbols denote stars with hydrogen being detected in their spectra, while open symbols refer to stars without hydrogen. The LMC stars analyzed in the present paper are represented by large symbols labeled by their "Brey" catalogue numbers (Breysacher 1981), while the smaller unlabeled symbols indicate the previously analyzed Galactic WN stars (Hamann & Koesterke 1998a).

of the panels of the fit diagrams (IUE short and long wavelength camera, respectively). The optical spectra have been normalized beforehand as described above.

In a first step, the observed spectra of each star were compared with synthetic spectra retrieved from our data bank of WN models (Hamann & Koesterke 1998a). Two grids (for v_∞ = 1600 km s^{-1} and 2500 km s^{-1}, respectively) are available, both for a uniform luminosity of $\log L/L_\odot = 5.3$ and $X_N = 1.5\%$ (nitrogen mass fraction, as adequate for the Galaxy). Those models are hydrogen-free, and clumping was not yet accounted for (i.e. $D = 1$).

After selecting the best-fitting models from the grid (which means, T_* and R_t being roughly determined), individual models were calculated for most of the program stars if appropriate. Especially, hydrogen was added to the composition for those stars with corresponding spectral signature (i.e. the He II lines blended with hydrogen Balmer lines being systematically stronger than the unblended He II lines of the Pickering series). Moreover, the terminal wind velocity is adjusted in the individual calculations. The radius is adequately chosen to avoid a scaling (i.e. we aim now at zero *shift*). The nitrogen mass fraction of $X_N = 0.8\%$ has been adopted for the LMC stars, but this reduction compared to the 1.5% typical for Galactic stars has no dramatic influence on the empirical parameters finally derived. An empirical determination of the nitrogen abundance will hardly become more accurate than by a factor of two, and is beyond the scope of the present paper.

The new models are generally calculated with a clumping factor of $D = 4$. If (unclumped) grid models are considered, the mass-loss rates are scaled down accordingly (cf. Hamann & Koesterke 1998b). We have not determined the clumping factors for each star individually. However, for none of the stars the comparison between observed and calculated spectra indicates an obvious discrepancy in the electron-scattering line wings. $D = 1$ (no clumping) would cause obvious differences, while clumping stronger than $D = 4$ could escape easy detection especially in spectra with only weak lines. Thus $D = 4$ seems to be a reasonable choice in general. But, as the derived $\dot{M}$ scales with $\sqrt{D}$ (Sect. 2.1), the uncertainty of the parameter D directly infers a corresponding error margin to the mass-loss rate.

5. Results and conclusions

The parameters for which the best fit of both continuum and line spectrum is achieved are compiled in Table 1. A subjective assessment of the fit quality (Column 15) should establish a relative reliability scale for these results. From the direct fit parameters we derive the "momentum ratio" (Column 13) which plays a crucial role in the discussion of radiation-driven stellar winds. While Br 85 shows an outstandingly high momentum ratio, 13 out of our 18 program stars have values between 0.8 and 6.3 and thus do not exceed the "single scattering limit" (i.e. unity) dramatically.

The stellar mass (Column 14) is estimated by using the mass-luminosity relation of Langer (1989) for the helium main sequence. Those stars with high hydrogen abundance might still gain part of their luminosity from a hydrogen-burning shell and thus actually can have much smaller masses.

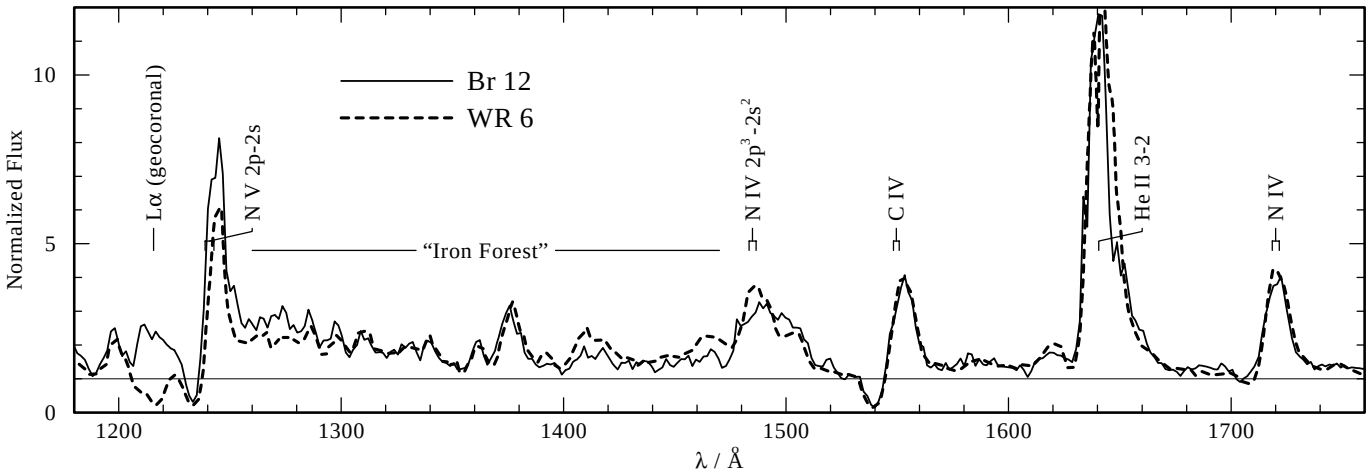

Fig. 3. Comparison between the observed, normalized spectra of Br 12 (LMC) and WR 6 (Galaxy) in the short-wavelength UV range (IUE-SWP). The stars appear as almost perfect spectroscopic twins. Helium, nitrogen and carbon lines as well as the "iron forest" are of very similar strength, not indicating any significant difference in metallicity.

Our present sample has five WNL stars in common with previous studies by Crowther et al. (1995a) and Crowther & Smith (1997). Their results differ from ours only marginally (e.g. by 0.1 in $\log L$, typically), which mutually confirms these independent analyses. Br 29 (the only WN/WC type in the sample) was also studied by Crowther et al. (1995b), who however arrived at significantly lower luminosity ($\log L$ = 5.0) than our result ($\log L$ = 5.8). This discrepancy is partly due to the higher stellar temperature we obtain, while a minor part comes from the higher interstellar reddening which we estimate from the continuum fit.

The locations of our program stars in the $\log T_*$-$\log R_\mathrm{t}$-plane are displayed in Fig. 2. Note that the transformed radius R_t scales inversely with the mass-loss rate (cf. Eq. (1)), i.e. higher R_t implies thinner winds. The late-type stars (WNL) have stellar temperatures of 30...40 kK and a considerable fraction of atmospheric hydrogen. The early subtypes (WNE) are hotter, up to 100 kK. The weak-lined WNE-w have larger values of R_t. Those stars with weakest winds show high hydrogen mass fractions, while the hotter and strong-lined WNE-s are free of hydrogen (except Br 56). Compared to their Galactic counterparts (small, unlabeled symbols in Fig. 2) there is no obvious difference in the parameters. Especially, the winds of the LMC stars seem not to be systematically weaker.

The close similarity between LMC and Galactic WN stars is demonstrated in Fig. 3 by comparing the observed spectra of Br 12 and WR 6. Both spectra are virtually identical (except of the stronger noise in the fainter LMC star) not only in the shown UV part, but also in the visual range. This perfect agreement holds for all spectral features, the helium, nitrogen and carbon lines as well as the "iron forest" (about 1260–1470 Å, produced by Fe V and Fe VI). Both stars also are of similar luminosity: $\log L/L_\odot$ = 5.3 and 5.4 for Br 12 and WR 6, respectively. The latter number (from Hamann & Koesterke 1998a), however, suffers from the distance uncertainly.

The existence of such Galactic–LMC spectroscopic twins is hard to understand, because of the lower metallicity in the LMC (about a factor of four for youngest stars, albeit presumably with large intrinsic scatter – cf. Holtzmann et al. 1999). Thus for Br 12 the metal lines should be weaker in relation to the helium lines, compared with WR 6. Moreover, if the WR winds are radiation-driven, the LMC star should also have a less dense wind. According to the basic work of Castor et al. (1975), $\dot{M}$ scales with the square root of the metallicity, roughly. This is more or less confirmed by detailed numerical models for radiation-driven O-star winds by, e.g., Haser et al. (1998) and other papers of the Munich group. Weaker winds of course produce smaller emission lines.

By test calculations (even with our most recent, iron line blanketed model code) we checked that both, an underabundance by a factor of four, and a decrease of mass-loss by a factor of two, would weaken the corresponding emission features significantly. Thus the close spectral similarity between WR 6 and Br 12 remains mysterious. The only consistent, but not very plausible solution is to adopt same metallicity for both stars.

Crowther (2000) recently studied the only known single WR star (Sk 41) in the SMC and found that, despite of the even lower metallicity environment, its stellar properties are typical of equivalent WN stars in the Galaxy and LMC.

Fig. 4 displays the results of our analyses in the Hertzsprung-Russell diagram. Note that the luminosities for the LMC stars under study are more reliable than for the Galactic stars (small unlabeled symbols in Fig. 3), because for the former the distance (of the LMC) is well known, while for the latter the distances are more or less uncertain. The figure also includes 15 more WNL stars (big unlabeled symbols) analyzed by Crowther et al. (1995a) and Crowther & Smith (1997). Again we see the WNE and WNL stars at their characteristic temperature ranges. Both subclasses cover a wide span of luminosities, Br 88 being the champion ($\log L/L_\odot$ = 6.5). The existence of many stars

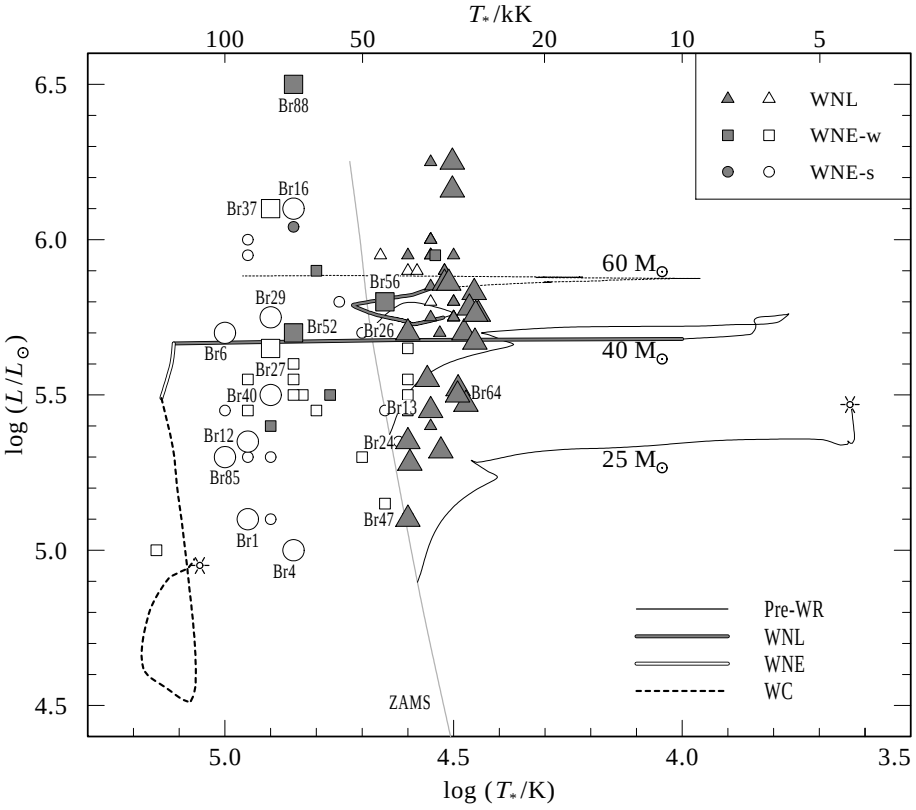

Fig. 4. Analyzed WN stars in the HRD. The big symbols labeled by the "Brey" number denote the LMC stars analyzed in this paper, augmented by WNL stars (unlabeled big triangles) analyzed by Crowther et al. (1995a) and Crowther & Smith (1997). Small, unlabeled symbols refer to Galactic objects (from Hamann & Koesterke 1998a). Filled and open symbols encode the presence and absence of atmospheric hydrogen, respectively. The Zero Age Main Sequence and theoretical tracks (25 and 40 $M_\odot$: from Schaller et al. 1992, set for $2 \times \dot{M}$; for 60 $M_\odot$: alternative track from Langer et al. 1994) are shown just for better orientation.

with comparably low luminosity down to $\log L/L_\odot$ = 5.0 (of both, hydrogen-containing WNL and hydrogen-free WNE type) puts rather stringent constraints to evolutionary scenarios. Let us emphasize once more that due to the known LMC distance those empirical luminosities are rather rigid facts and not so much model dependent. Standard evolutionary tracks for single stars do not lead to WN stars of such low luminosities and correspondingly small core masses. However, rotationally induced mixing can produce relatively faint hydrogen-containing and hydrogen-free WN stars (Fliegner & Langer 1995).

The mass-loss rates are plotted versus luminosity in Fig. 5 on logarithmic scales. If we expected a close correlation (as found for OB stars), the result is disappointing. A linear regression analysis to the total LMC sample gives a_1 = -5.69 and a_2 = 0.20, for the coefficients in

$$\log \frac{\dot{M}}{M_\odot\ \mathrm{yr}^{-1}} = a_1 + a_2 \log \frac{L}{L_\odot}\ , \qquad (2)$$

but the standard deviation from that relation is as large as ± 0.36 in $\log \dot{M}$. This is hardly better than adopting a mean mass-loss rate independent of L ($\log \dot{M} = -4.57 \pm 0.37$).

The scatter from any simple $\dot{M}$–L–relation is much bigger than our estimate of the (random) error in the empirical data. Obviously, the manifold of WN stars cannot be represented as a function of only one parameter. E.g., the late-type (WNL) and weak-lined early-type (WNE-w) stars have on the average lower mass-loss than the strong-lined early subtypes (WNE-s). The full-drawn straight line in Fig. 5 is the least-square fit to the WNE-s stars in our LMC sample (a_1 = -8.28, a_2 = 0.70).

We investigated if a more-dimensional linear regression would result in a better representation of the data. In a previous paper (Hamann et al. 1995) we suggested that there is gradual increase from OB-type mass-loss rates to the much higher WR mass-loss rates which is correlated with the hydrogen abundance. A linear regression after augmenting Eq. (2) by a further term $a_3 X_\mathrm{H}$ confirms that trend, but did not result in a convincingly better representation of the data. We also considered $\dot{M}$ as linear function of $\log L$ and $\log T_*$, but obtained no better correlation.

In principal, part of the scatter in Fig. 5 might be attributed to a scatter in the clumping factor D which we keep constant here and which enters the mass-loss rate determination. However, there is no obvious evidence for D being extremely different for the individual stars (cf. end of Sect. 4). Moreover, one would expect that the clumping factor is somehow related to the fundamental stellar parameters as well.

Thus we must conclude that stars of same luminosity can have largely different mass-loss rates even if hydrogen abundance and effective temperature are similar. The (possibly large) scatter in individual metallicities might provide an explanation which could be tested when future analyses become more accurate by improved (e.g. line-blanketed) models and better observations.

In Fig. 5 we include the Galactic stars (small unlabeled symbols) which we had analyzed previously (Hamann & Koesterke 1998a) by basically the same technique, except of the clumping effect. In order to account for the latter, we have scaled down the mass-loss rates by a factor of two according to the same

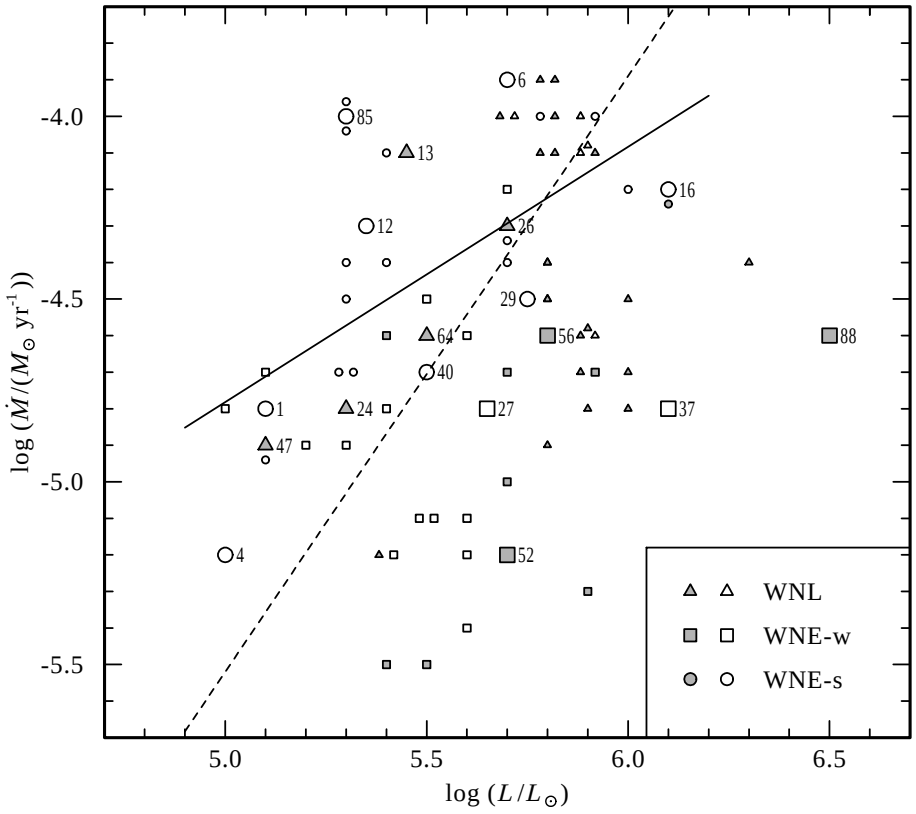

Fig. 5. Mass-loss rates versus luminosity. The big symbols labeled by their "Brey" catalogue numbers denote our LMC program stars. The smaller, unlabeled symbols refer to the Galactic WN sample taken from Hamann & Koesterke (1998a), but after diminishing the mass-loss rate by a factor of two in order to account for the same clumping (density enhancement $D = 4$) as adopted in the present study. Filled or open symbols denote stars with and without detectable hydrogen, respectively, while the symbol shape distinguishes the spectral subgroups (see inlet). The full line is a linear regression to the strong-lined, hydrogen-free LMC stars (WNE-s), while the dashed line gives the corresponding relation found by Nugis & Lamers (2000).

Table 2. Carbon abundances for some of the program stars

Brey	Spectral subtype†		X_C
	Smith 68	SSM 96	[%]
(1)	(2)	(3)	(4)
12	WN4-s	WN4b	0.015
24	WN7	WN6h	0.01
29	WN3/CE-s	WN4b/CE	1
88	WN4.5-w+abs	WN5+B?	0.03

† For classifications cf. footnote of Table 1

density enhancement ($D = 4$) as adopted in the present study. The average mass-loss rate and the scatter of the Galactic stars do not differ significantly from our LMC sample, in contrast to the expected metallicity effects.

Note that the steep correlation ($a_1 = -13.67$, $a_2 = 1.60$ for zero hydrogen – dashed line in Fig. 5) found by Nugis & Lamers (2000) for the Galactic stars (on the basis of a few radio-emission measurements augmented by further spectroscopic $\dot{M}$ estimates) is not confirmed by a statistical analysis of our data, although the by-eye comparison reveals that it also roughly fits within the given scatter.

For four of our program stars we determined the carbon abundance (cf. Table 2) by including this element in our model calculations. For the "normal" WN subtypes the obtained carbon mass fractions ($1...3\ 10^{-4}$) compare well with the expected equilibrium value in CNO processed material. The much stronger carbon lines in the WN/WC type star Br 29 can be consistently explained by a single-star model of enhanced carbon abundance. The mass fraction is almost two orders of magnitude higher than in WN stars (about 1% per mass). This confirms the finding by Crowther et al. (1995b), although they arrived at a somewhat smaller value (0.3% carbon mass fraction). The existence of carbon-enhanced WN stars (cf. WR 8 in the Galactic sample) allows conclusions about the efficiency of internal mixing processes during the evolution of massive stars, as has been discussed by Langer (1991).

As we have shown, our models reproduce the observed WN spectra when the model parameters are suitably adjusted. The 18 LMC stars of our sample largely differ in their spectral appearance, mainly with respect to the observed ionization stages and emission line strengths. Correspondingly, the obtained parameters (luminosities, mass-loss rates etc.) show a complex variety without simple correlations. Systematic differences between the Galactic WN stars and our LMC sample are not evident, i.e. the expected metallicity effects are not confirmed.

References

Breysacher J., 1981, A&AS 43, 203
Castor J.I., Abbott D.C., Klein R.I., 1975, ApJ 195, 157
Conti P.S., Massey P., 1989, ApJ 337, 251
Cowley A.P., Crampton D., Hutchings J.B., Thompson I.B., 1984, PASP 96, 968
Crowther P.A., 2000, A&A 356, 191
Crowther P.A., Smith L.J., 1997, A&A 320, 500
Crowther P.A., Hillier D.J., Smith L.J., 1995a, A&A 293, 172
Crowther P.A., Smith L.J., Willis A.J., 1995b, A&A 304, 269

Fliegner J., Langer N., 1995, In: van der Hucht K.A., Williams P.M. (eds.) Wolf-Rayet Stars: Binaries, Colliding Winds, Evolution. Proc. IAU Symp. 163, p. 326
Gräfener G., Hamann W.-R., Koesterke L., 2000, In: Lamers H.J.G.L.M., Sapar A. (eds.) Thermal and Ionization Aspects of Flows from Hot Stars: Observations and Theory. ASP Conference Series in press
Hamann W.-R., Koesterke L., 1998a, A&A 333, 251
Hamann W.-R., Koesterke L., 1998b, A&A 335, 1003
Hamann W.-R., Leuenhagen U., Koesterke L., Wessolowski U., 1992, A&A 255, 200
Hamann W.-R., Koesterke L., Wessolowski U., 1993, A&A 274, 397
Hamann W.-R., Wessolowski U., Koesterke L., 1994, A&A 281, 184
Hamann W.-R., Koesterke L., Wessolowski U., 1995, A&A 299, 151
Haser S.M., Pauldrach A.W.A., Lennon D.J., et al., 1998, A&A 330, 285
Hillier D.J., 1984, ApJ 280, 744
Hillier D.J., 1987a, ApJS 63, 947
Hillier D.J., 1987b, ApJS 63, 965
Hillier D.J., Miller D.L., 1998, ApJ 496, 407
Holtzmann J.A., Gallagher J.S., Cole A.A., et al., 1999, ApJ 118, 2279
Howarth J.D., 1983, MNRAS 203, 301
Koesterke L., Hamann W.-R., Schmutz W., Wessolowski U., 1991, A&A 248, 166
Koesterke L., Gräfener G., Hamann W.-R., 2000, In: Lamers H.J.G.L.M., Sapar A. (eds.) Thermal and Ionization Aspects of Flows from Hot Stars: Observations and Theory. ASP Conference Series in press
Langer N., 1989, A&A 210, 93
Langer N., 1991, A&A 248, 531
Langer N., Hamann W,-R., Lennon M., et al., 1994, A&A 290, 819
Madore B.F., Freedman W.L., 1998, ApJ 492, 110
Nugis T., Lamers H.J.G.L.M., 2000, A&A submitted
Schaller G., Schaerer D., Meynet G., Maeder A., 1992, A&AS 96, 269
Schmutz W., 1997, A&A 321, 268
Schmutz W., Hamann W.-R., Wessolowski U., 1989, A&A 210, 236
Seaton M.J., 1979, MNRAS 187, 73P
Smith L.F., 1968, MNRAS 140, 409
Smith L.F., Shara M.M., Moffat A.F.J., 1996, MNRAS 281, 163
Torres-Dodgen A.V., Massey P., 1988, AJ 96, 1076